CHEMICAL PHYSICS

Encoding of vinylidene isomerization in its anion photoelectron spectrum

Jessalyn A. DeVine,[1]* Marissa L. Weichman,[1]* Benjamin Laws,[2] Jing Chang,[3] Mark C. Babin,[1] Garikoitz Balerdi,[4] Changjian Xie,[5] Christopher L. Malbon,[6] W. Carl Lineberger,[7] David R. Yarkony,[6] Robert W. Field,[8] Stephen T. Gibson,[2] Jianyi Ma,[3]† Hua Guo,[5] Daniel M. Neumark[1,9]†

Vinylidene-acetylene isomerization is the prototypical example of a 1,2-hydrogen shift, one of the most important classes of isomerization reactions in organic chemistry. This reaction was investigated with quantum state specificity by high-resolution photoelectron spectroscopy of the vinylidene anions H_2CC^- and D_2CC^- and quantum dynamics calculations. Peaks in the photoelectron spectra are considerably narrower than in previous work and reveal subtleties in the isomerization dynamics of neutral vinylidene, as well as vibronic coupling with an excited state of vinylidene. Comparison with theory permits assignment of most spectral features to eigenstates dominated by vinylidene character. However, excitation of the ν_6 in-plane rocking mode in H_2CC results in appreciable tunneling-facilitated mixing with highly vibrationally excited states of acetylene, leading to broadening and/or spectral fine structure that is largely suppressed for analogous vibrational levels of D_2CC.

The 1,2-hydrogen shift is the simplest bond-breaking isomerization reaction in organic chemistry (*1*), and the prototypical example of this process is the isomerization of vinylidene (H_2CC) to acetylene (HCCH). Vinylidene, the smallest unsaturated carbene (*2*), has been implicated as a transient intermediate in many chemical processes (*3*–*6*) but is of particular interest as a high-energy form of acetylene (*7*). From the perspective of chemical physics, the $H_2CC \rightleftharpoons$HCCH isomerization (Fig. 1) is a benchmark unimolecular reaction; the small number of atoms allows application of sophisticated theoretical methods to describe the isomerization dynamics (*8*–*13*), and the interplay between theory and experiment has provided a great deal of insight into this reaction (*14*, *15*). The low barrier (~0.1 eV) (Fig. 1) for vinylidene isomerization (*8*, *10*) can lead to extensive tunneling interactions with acetylene states, and over the past several decades considerable effort has been invested in probing this isomerization from both sides of the barrier. On the acetylene side, Field and co-workers (*15*, *16*) have searched for spectroscopic signatures of vinylidene in highly vibrationally excited levels of HCCH, where the minimum-energy isomerization path lies along the local-bending vibrational coordinates. Alternatively, the vinylidene well can be accessed directly by photodetachment of the vinylidene anion (H_2CC^-), and several research groups have used this approach to probe the spectroscopy and dynamics of neutral H_2CC (*17*–*21*).

Previous photodetachment-based experiments have led to differing views regarding the time scale on which vinylidene isomerizes to acetylene. In an anion photoelectron spectroscopy study, Ervin *et al.* (*18*) observed that transitions to the $\tilde{X}^1A_1$ state of H_2CC were considerably broader than those arising from detachment to the higher-lying $\tilde{a}^3B_2$ state, for which the barrier to isomerization is considerably larger. The extra broadening of ground-state band features was attributed to isomerization on a subpicosecond time scale. In contrast, later Coulomb explosion imaging (CEI) experiments by Vager and colleagues (*19*) indicated that neutral H_2CC formed by anion photodetachment is stable on at least a microsecond time scale. It should be noted that "lifetime" is an ill-defined concept in such a system, because both acetylene and vinylidene are bound species whose eigenstates cannot form a true continuum. However, individual eigenstates may have varying degrees of mixing between zeroth-order states of the two isomers, especially near and above the isomerization barrier. This mixing has been explored in quantum dynamical simulations of the anion photoelectron spectrum starting with work by Bowman and colleagues (*10*), who found the simulated spectrum to be dominated by sharp peaks associated with isolated vinylidene eigenstates.

The aim of the current work was to experimentally characterize individual vibrational eigenstates of vinylidene and to understand the vibrational mode dependence of mixing with acetylene. To this end, we measured photodetachment spectra of H_2CC^- and D_2CC^- anions at higher resolution than previous work (*18*), using two complementary experimental methods, high-resolution photoelectron imaging (HR-PEI) (*22*), and slow electron velocity-map imaging of cryogenically cooled anions (cryo-SEVI) (*23*). The experiments are supplemented by full-dimensional quantum dynamics calculations on a highly accurate ab initio–based potential energy surface, carried out previously for the H_2CC-HCCH system (*12*, *24*) and expanded here by covering larger sections of configuration space in both isomeric regions.

The combination of experiment and theory shows that photodetachment directly accesses eigenstates that are mostly localized in the vinylidene well. The H_2CC and D_2CC isotopologues both undergo vibronic coupling to a high-lying vinylidene electronic state, which results in the appearance of nominally Franck-Condon (FC) forbidden transitions to neutral vibrational levels, with excitation of non–totally symmetric (b_2) modes. Most notable is the vibronic coupling–induced observation of features involving odd quanta of excitation in the in-plane rocking (ν_6) mode, which, for the H_2CC isotopologue, mixes strongly with the local-bending modes in the acetylene well. Isomerization is largely encoded in the spectra of vibrational states that involve excitation of this mode.

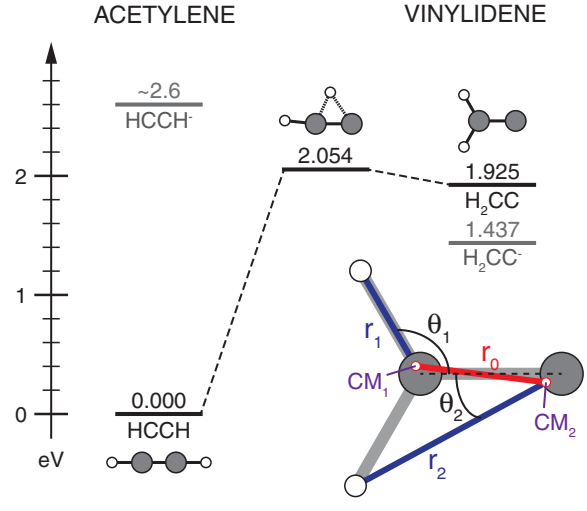

Fig. 1. Energy diagram for the neutral vinylidene-acetylene isomerization. Energies (in eV, relative to HCCH) and geometries were obtained from (*21*). Experimental energies for the anions of both isomers are shown in gray; the H_2CC^- value was obtained from the present work, whereas the $HCCH^-$ value was estimated from electron-scattering experiments (*28*). The CH–CH Jacobi coordinate system used to describe the isomerization is shown as an inset.

[1]Department of Chemistry, University of California, Berkeley, CA 94720, USA. [2]Research School of Physics and Engineering, Australian National University, Canberra, ACT 2601, Australia. [3]Institute of Atomic and Molecular Physics, Sichuan University, Chengdu, Sichuan 610067, China. [4]Departmento de Química Física, Facultad de Ciencias Químicas, Universidad Complutense de Madrid (Unidad Asociada I+D+I CSIC), 28040 Madrid, Spain. [5]Department of Chemistry and Chemical Biology, University of New Mexico, Albuquerque, NM 87131, USA. [6]Department of Chemistry, Johns Hopkins University, Baltimore, MD 21218, USA. [7]JILA and Department of Chemistry and Biochemistry, University of Colorado, Boulder, CO 80309, USA. [8]Department of Chemistry, Massachusetts Institute of Technology, Cambridge, MA 02139, USA. [9]Chemical Sciences Division, Lawrence Berkeley National Laboratory, Berkeley, CA 94720, USA.
*These authors contributed equally to this work.
†Corresponding author. Email: majianyi81@163.com (J.M.); dneumark@berkeley.edu (D.M.N.)

The experiments reported here used velocity-map imaging (VMI) detection schemes to measure the electron kinetic energy (eKE) distribution and photoelectron angular distribution (PAD) that result from electron photodetachment of mass-selected anions. The VMI spectrometer used in the HR-PEI measurements (fig. S1) was optimized to provide 0.7 to 25 cm^{-1} resolution over a wide range of eKE, so that measurements at a single photon energy ($h\nu$) could be used to obtain vibrationally resolved spectra with reliable intensities and PADs. The cryo-SEVI spectrometer (fig. S2) provided higher resolution (sub-meV) over a narrower range of eKEs, assisted by cooling the anions to ~10 K before detachment to reduce spectral congestion arising from anion rotational and vibrational excitation. Together, the HR-PEI and cryo-SEVI techniques yield a more complete picture of the photoelectron eKE spectrum and PADs than when used separately.

The cryo-SEVI spectra of H_2CC^- and D_2CC^- (Fig. 2A) and the HR-PEI spectrum of H_2CC^- (Fig. 2B) display photoelectron intensity versus electron binding energy (eBE), where eBE = $h\nu$ − eKE. All three spectra are dominated by the vibrational origin (A) and show transitions to vibrational levels up to ~4000 cm^{-1} above the vinylidene vibrational ground state. PADs are readily obtained from photoelectron images [supplementary materials (SM), section B], an example of which is shown in Fig. 2B. For each peak, the PADs yield the anisotropy parameter (β), which by definition falls between –1 and 2. These limits correspond to perpendicular and parallel detachment, respectively (*25*). Figure 2C shows β for several peaks as a function of eKE, obtained from HR-PEI measurements at several photon energies. The PADs extracted from the cryo-SEVI spectra (fig. S3) are in agreement with the HR-PEI results; with the exception of features B, I, and K, all peaks in the cryo-SEVI spectra of both isotopologues have $\beta < 0$ for eKEs below 1 eV, and peaks B, I, and K show distinctly positive β values at these kinetic energies.

The enhanced resolution of cryo-SEVI is evident in the considerably narrower linewidths in Fig. 2A compared with previous photoelectron spectra (*18*), and a direct comparison is shown in fig. S4. The linewidths of the vibrational origins and most of the other peaks are ~10 cm^{-1} and ~30 cm^{-1} in the H_2CC^- and D_2CC^- spectra, respectively, suggesting that these features are predominantly transitions that terminate in single eigenstates. These linewidths are primarily determined by the underlying rotational contours (fig. S5) and, as discussed previously (*21*) and in section C of the SM, reflect the differing nuclear spin statistics for H and D atoms. In contrast to the previously published spectrum, the majority of features do not display appreciable broadening relative to the previously observed excited state features (*21*). However, there are several anomalously broadened and irregular regions (B, C, and I) in the H_2CC^- cryo-SEVI spectrum, discussed in more detail below.

Comparison with the theoretical spectra in Fig. 2A (red traces) and figs. S6 and S7 allows unambiguous assignment of nearly all experimentally observed peaks, as shown in Table 1. These assignments are particularly clear for D_2CC, where discrepancies between theory and experiment are <10 cm^{-1} for all features, excluding peak G. From the rotational contours of the 0_0^0 bands, we obtain electron affinities (EAs) of 0.4866(8) and 0.488(2) eV for H_2CC and D_2CC, respectively, as described in section C of the SM. These EAs lie within the error bars of the previously reported values (*18*) of 0.490(6) and 0.492(6) eV, respectively; they reflect our enhanced resolution and the ability to partially resolve the rotational structure of the band origins. Most of the remaining features in the two spectra can be attributed to FC-allowed transitions involving totally symmetric (a_1) neutral vibrational levels, which, within the Born-Oppenheimer approximation, are the only transitions that can appear in the theoretical spectra for detachment from the anion vibrational ground state. Features B and I are nominally assigned to the FC-forbidden 6_0^1 and mixed 5_0^1 and $1_0^1 6_0^1$ transitions, both involving b_2-symmetric vibrational levels of neutral vinylidene.

These FC-forbidden transitions are attributed to Herzberg-Teller (HT) coupling to an excited electronic state with B_2 symmetry (SM sections B and C). The $\tilde{B}^1B_2$ state has been predicted to lie about 4 eV above the $\tilde{X}^1A_1$ state (*26*). We have observed detachment to this state (fig. S8), finding its term energy to be T_0 = 3.997(3) eV with respect to the $\tilde{X}^1A_1$ state and its anisotropy parameter to be positive. The derivative coupling between the $\tilde{X}^1A_1$ and $\tilde{B}^1B_2$ states has been calculated near

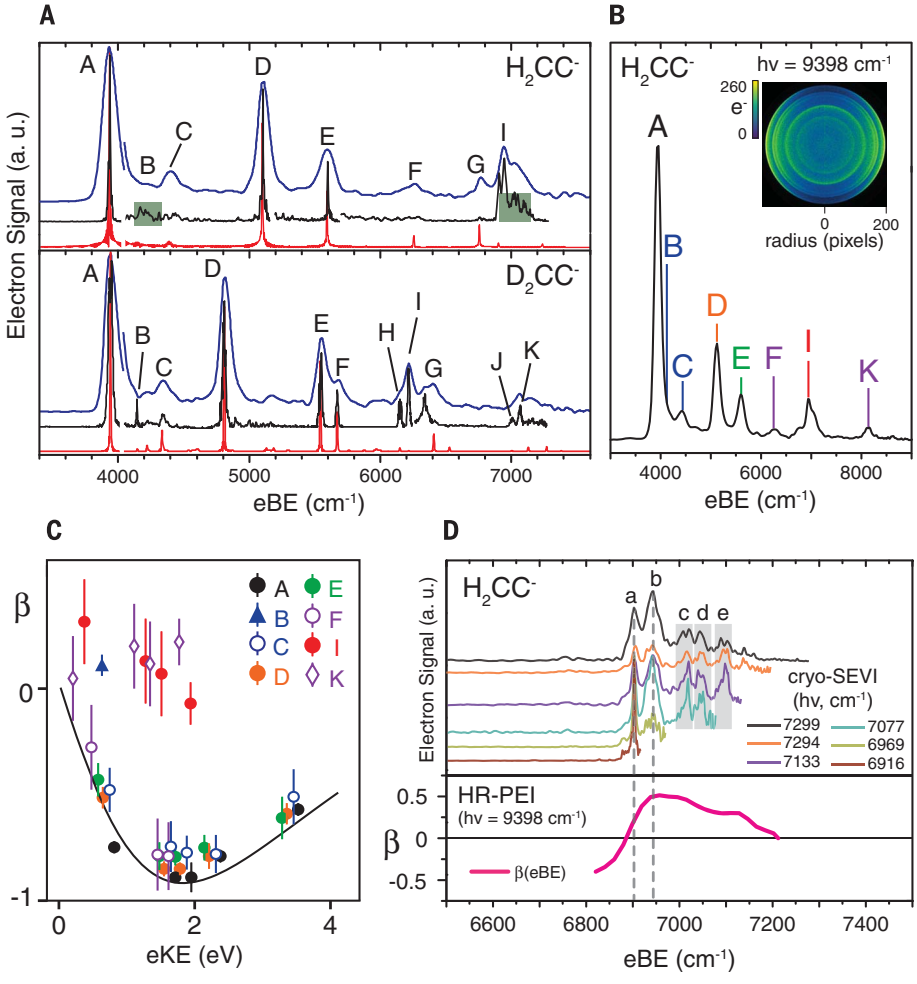

Fig. 2. Vinylidene photoelectron spectra. (**A**) Cryo-SEVI spectra of H_2CC^- (top) and D_2CC^- (bottom), as well as theoretical results for both isotopologues (red). The blue traces represent overview spectra, and the black traces are higher-resolution composite spectra; see section A of the SM for more details. For clarity, all traces have been scaled by a factor of 2 following the break in the overview after peak A. (**B**) HR-PEI spectrum of H_2CC^-. The image used to construct the spectrum is shown as an inset. (**C**) PADs of various spectral features obtained from the HR-PEI H_2CC^- spectrum. The solid line shows a Hanstorp p-orbital detachment fit to the anisotropy parameter of peak A (*29*). Error bars correspond to one standard deviation of the anisotropy parameter obtained from the fitting process. (**D**) Region I of the H_2CC^- photoelectron spectrum, showing the underlying structure revealed by cryo-SEVI. The anisotropy parameter obtained from the HR-PEI spectrum is also shown to illustrate the variation in angular distribution across this region. Vertical dashed lines show how peaks a and b line up with the anisotropy parameter. Plotted data are available in the supplementary materials.

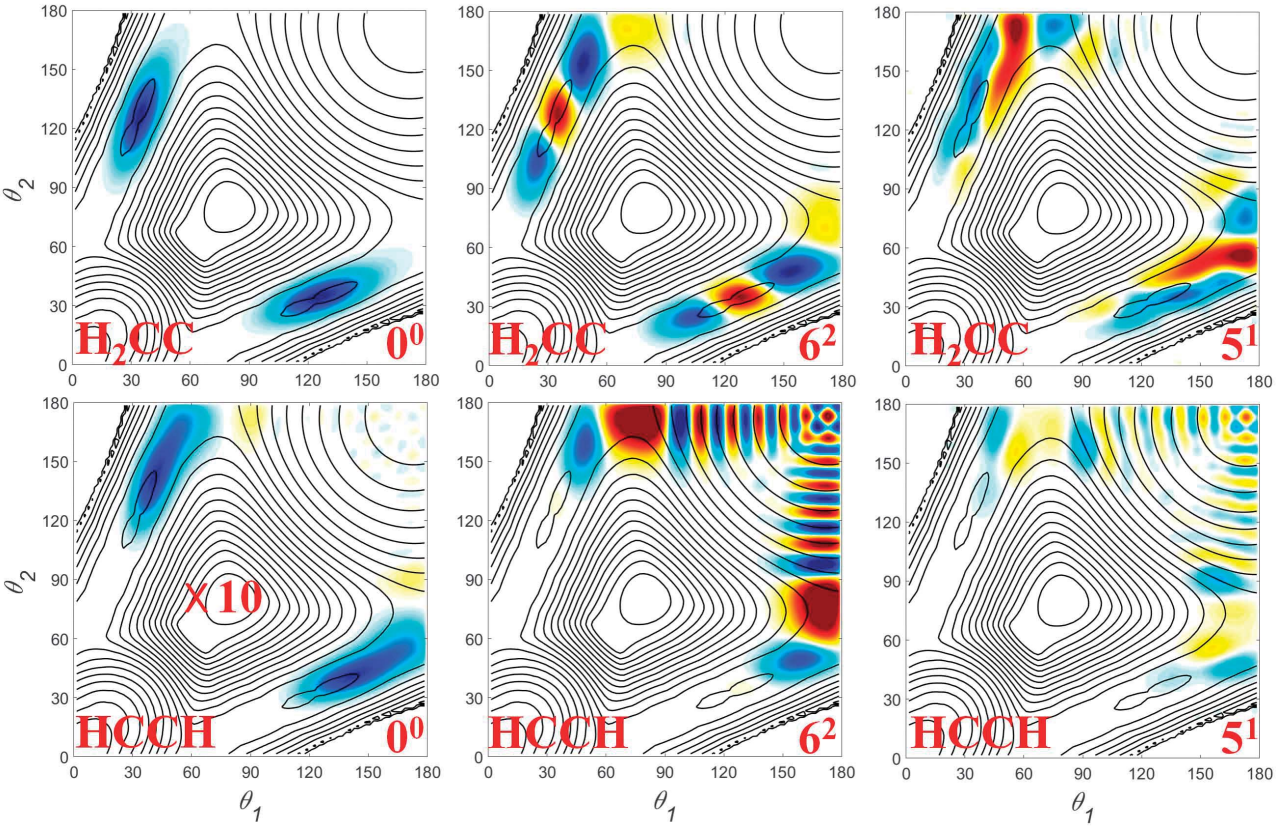

Fig. 3. Calculated wave functions for neutral vibrational levels of H_2CC. Wave functions of the 0^0, 6^2, and 5^1 states are shown along the θ_1 and θ_2 directions of the CH–CH Jacobi coordinates, with the coordinate r_0 taking the equilibrium value of H_2CC (top) or HCCH (bottom) and the wave functions summed over the remaining coordinates. The acetylene component is dominated by local-bender states along the θ_1, θ_2 ~ 180° axes. The two-dimensional potential energy surface is superimposed, in which the $\theta_1 = \theta_2 = 180°$ well corresponds to HCCH.

the vinylidene minimum (SM section E), and the interaction between these states is found to be localized largely along the ν_6 mode, with a minor contribution from the ν_5 mode. Peaks B and I also exhibit positive anisotropy parameters (Fig. 2C), in contrast to all of the FC-allowed features, consistent with HT coupling between the two electronic states (*27*). Moreover, as discussed in section C of the SM, the rotational selection rules for photodetachment differ for the FC-allowed ($\Delta K_a = \pm 1$) versus HT-allowed ($\Delta K_a = 0$) transitions, leading to the narrower rotational profiles of peaks B and I (7 and 16 cm^{-1} full width at half maximum, respectively) in the D_2CC^- SEVI spectrum relative to the FC-allowed transitions.

Overall, the D_2CC^- cryo-SEVI spectrum is what would be expected for a well-behaved, stable molecule, albeit one that exhibits HT coupling with an excited electronic state. The same is true for much of the H_2CC^- spectrum, with the exception of features B, C, and I. Features B and C, assigned to the 6_0^1 and 6_0^2 transitions, appear in the cryo-SEVI spectrum as broad, weak features, even at high resolution (black trace, Fig. 2A). The spectral broadening indicates participation of multiple eigenstates, each of which carries some vinylidene oscillator strength. Figure 2D shows that feature I, in the vicinity of the calculated 5_0^1 and $1_0^1 6_0^1$ transitions, resolves into a cluster of five closely spaced, narrow peaks (a to e, binding energies in table S1). Comparison with the HR-PEI angular distribution reveals notable variation in the anisotropy parameter across this series of peaks, with a considerably lower β value for peak a than peaks b to e. In addition, the intensity of peak a decreases more slowly than the other features as the photon energy is lowered. Both observations indicate variation of the partial wave contributions to photodetachment across region I, suggesting that the electronic characters of the final eigenstates are highly variable.

To understand how the isomerization mechanism is encoded in the neutral eigenstates, and to gain additional insights into the experimental spectra, we turn to the calculated wave functions for the lowest two FC-allowed vibrational eigenstates populated by photodetachment of H_2CC^- anions (0^0 and 6^2) and a state allowed only by HT coupling (5^1). Using the CH–CH Jacobi coordinates shown in the inset of Fig. 1, the wave functions are plotted in Fig. 3, superimposed on a contour plot of the potential energy surface. In the top and bottom panels, the distance between CH centers of mass (r_0) is constrained to either the vinylidene or acetylene equilibrium value, respectively, so that the bending wave functions are shown for both the vinylidene and acetylene wells. For the ground vinylidene state (0°), there is very little acetylene character, indicating strong localization in the vinylidene well. However, excitation of the in-plane rocking mode of vinylidene (6^2) introduces appreciable acetylene character, featuring highly excited states in the local-bending coordinates (local benders), evidenced by the large number of nodes along the angular coordinates (θ_1, θ_2) (*15*).

The plots in Fig. 3 and fig. S9 also show that the neutral 5^1 state mixes with the $1^1 6^1$ state through an anharmonic interaction, giving region I its intensity through the ν_6-dominated HT coupling. This interaction is enhanced by the energy lowering of the $1^1 6^1$ state relative to the sum of the ν_1 and ν_6 fundamentals, due to the strong intermode anharmonicity between the stretching and rocking modes. The other peaks in feature I could be due to higher b_2 states, such as $5^1 6^2$ and other nearby FC-allowed transitions.

Figure 3 shows that this mixed $5^1 \sim 1^1 6^1$ state exhibits appreciable acetylene character along the local-bending coordinates, with similar nodal structure as is seen for the 6^2 state. This result links the spectroscopy of vinylidene to its isomerization dynamics; the minimum-energy isomerization pathway follows the rocking normal mode of vinylidene, which ultimately connects with the local-bending vibrational states of acetylene. Indeed, the acetylenic contributions to the 6^2 and $5^1 \sim 1^1 6^1$ eigenfunctions involve strong admixtures of the local-bending excitation, which has been extensively probed by spectroscopic studies of highly excited acetylene (*15*). For D_2CC, the

Table 1. Peak positions (cm^{-1}), experimental and theoretical shifts from the vibrational origin (cm^{-1}), and assignments for the H_2CC^- and D_2CC^- ground-state photoelectron spectra. Shifts were extracted from the cryo-SEVI scans, and HR-PEI peak positions for H_2CC^- are shown for comparison. Cryo-SEVI peak positions were extracted from the high-resolution (black) traces in Fig. 2A unless otherwise noted. Uncertainties in peak positions correspond to 1 σ, obtained from a Gaussian fit to the experimental trace. Theo., theoretical.

	H_2CC^-					D_2CC^-				Assignment
Peak	HR-PEI eBE	cryo-SEVI eBE	Shift	Theo.	H_2CC%	cryo-SEVI eBE	Shift	Theo.	D_2CC%	
A	3940(60)	3935(7)	0	0.0	100	3941(17)	0	0.0	100	0_0^0
B	–	4190(50)*	255	283.2	84	4143(3)	202	203.9	100	6_0^1
C	4400(90)	4402(52)†	470	454.1	58	4345(18)	404	396.8	98	6_0^2
D	5120(60)	5103(5)	1168	1166.0	97	4809(11)	868	868.6	100	3_0^1
E	5570(50)	5597(4)	1662	1659.6	97	5547(10)	1606	1601.8	99	2_0^1
F	6250(80)	6240(70)†	2305	2322.6	96	5671(8)	1730	1730.0		3_0^2
G	6740(70)	6780(60)†	2845	2822.0	97	6339(18)	2398	2468.0		$2_0^1 3_0^1$
H				2967.7		6152(12)	2211	2206.7		1_0^1
I	6950(50)	6943(12)‡	3008	3013.7	82	6216(7)	2275	2276.9	99	5_0^1
				3117.6	68			2389.9	95	$1_0^1 6_0^1$
J						7008(14)	3067	3059.7		$1_0^1 3_0^1$
K	8130(70)	8125(41)†	4190	4218.4		7065(12)	3124	3125.5		$3_0^1 5_0^1$

*Peak position obtained by fitting the highlighted region B in Fig. 2A to a single Gaussian. †These features did not maintain sufficient intensity near-threshold to appear in high-resolution cryo-SEVI scans, and thus the eBEs are obtained from the lower-resolution overview scans (blue traces) in Fig. 2A. ‡Reported position corresponds to feature b in Fig. 2D.

extent of mixing with DCCD is negligible, presumably owing to the much narrower eigenfunctions resulting in suppressed tunneling. The wave functions for other H_2CC and D_2CC states can be found in figs. S9 to S11.

Chemically, isomerization entails the breaking and formation of bonds within a molecule. To understand the dynamics of the 1,2-hydrogen shift in this system, one needs to quantum mechanically simulate transitions between various vibrational eigenstates that have different amplitudes of the zeroth-order vinylidene (^{1}) and acetylene (^{2}) basis states: $\Psi_n^{(neutral)} \approx c_n^{(1)}\psi_n^{(1)} + c_{nm}^{(2)}\psi_m^{(2)}$. The extent of mixing, which encodes the isomerization, depends on the energy difference between $\psi_n^{(1)}$ and $\psi_m^{(2)}$, as well as the strength of the interaction matrix element between the two. As mentioned above, the acetylene states involved in the mixing ($\psi_m^{(2)}$) are mostly the local benders, which have a much smaller density of states than the total density of acetylene vibrational states. The spectral intensity of a peak in the photoelectron spectrum is primarily determined by $I_n \approx \left|c_n^{(1)}\right|^2 \left|\left\langle \psi_n^{(1)} \middle| \Psi^{(anion)} \right\rangle\right|^2$. The vinylidene weights, $\left|c_n^{(1)}\right|^2$, can be approximately extracted from the calculated H_2CC and D_2CC eigenfunctions and are listed in Table 1. For H_2CC, only those final states with ν_6 excitation mix strongly with HCCH, whereas for D_2CC, the mixing with DCCD is much smaller due to the more confined wave functions.

The cryo-SEVI and HR-PEI spectra, with the supporting theoretical analysis, offer insights into the vinylidene-acetylene isomerization and its influence on the vinylidene photoelectron spectrum. Most neutral vibrational states formed via photodetachment are dominated by vinylidene character for both isotopologues, an observation consistent with the main conclusion of the CEI experiment (*19*) and the calculations by Bowman and colleagues (*10*). However, H_2CC states in which the ν_6 mode is excited show non-negligible acetylene character, which manifests as spectral broadening and/or fine structure for this isotopologue. Excitation of this mode can occur through FC-allowed transitions (6^2), vibronic coupling via an excited state of vinylidene (6^1), or anharmonic coupling between ground state vibrational levels ($5^1 \sim 1^1 6^1$). This spectroscopic result implies that in the range of excitation energies probed here, the isomerization of vinylidene to acetylene is highly state-specific and is promoted by excitation of the ν_6 mode. Considerably less coupling to acetylene is observed for D_2CC, which suggests that isomerization of D_2CC is considerably less facile even when the ν_6 mode is excited. These insights provide a quantum mechanical foundation for understanding the 1,2-hydrogen shift reaction.

REFERENCES AND NOTES

1. Y. Yamamoto, S. I. Murahashi, I. Moritani, *Tetrahedron* **31**, 2663–2667 (1975).
2. P. J. Stang, *Chem. Rev.* **78**, 383–405 (1978).
3. P. S. Skell, J. E. Villaume, F. A. Fagone, *J. Am. Chem. Soc.* **94**, 7866–7867 (1972).
4. A. H. Laufer, *J. Chem. Phys.* **73**, 49–52 (1980).
5. M. M. Hills, J. E. Parmeter, W. H. Weinberg, *J. Am. Chem. Soc.* **109**, 4224–4232 (1987).
6. M. Ahmed, D. S. Peterka, A. G. Suits, *J. Chem. Phys.* **110**, 4248–4253 (1999).
7. J. Zádor, M. D. Fellows, J. A. Miller, *J. Phys. Chem. A* **121**, 4203–4217 (2017).
8. T. Carrington Jr., L. M. Hubbard, H. F. Schaefer III, W. H. Miller, *J. Chem. Phys.* **80**, 4347–4354 (1984).
9. R. L. Hayes, E. Fattal, N. Govind, E. A. Carter, *J. Am. Chem. Soc.* **123**, 641–657 (2001).
10. S. Zou, J. M. Bowman, A. Brown, *J. Chem. Phys.* **118**, 10012–10023 (2003).
11. H. Lee, J. H. Baraban, R. W. Field, J. F. Stanton, *J. Phys. Chem. A* **117**, 11679–11683 (2013).
12. H. Han, A. Li, H. Guo, *J. Chem. Phys.* **141**, 244312 (2014).
13. Y. Ren, W. Bian, *J. Phys. Chem. Lett.* **6**, 1824–1829 (2015).
14. J. K. Lundberg *et al.*, *J. Chem. Phys.* **98**, 8384–8391 (1993).
15. M. P. Jacobson, R. W. Field, *J. Phys. Chem. A* **104**, 3073–3086 (2000).
16. M. P. Jacobson, J. P. O'Brien, R. W. Field, *J. Chem. Phys.* **109**, 3831–3840 (1998).
17. S. M. Burnett, A. E. Stevens, C. S. Feigerle, W. C. Lineberger, *Chem. Phys. Lett.* **100**, 124–128 (1983).
18. K. M. Ervin, J. Ho, W. C. Lineberger, *J. Chem. Phys.* **91**, 5974–5992 (1989).
19. J. Levin *et al.*, *Phys. Rev. Lett.* **81**, 3347–3350 (1998).
20. H. K. Gerardi *et al.*, *J. Phys. Chem. A* **114**, 1592–1601 (2010).
21. J. A. DeVine *et al.*, *J. Am. Chem. Soc.* **138**, 16417–16425 (2016).
22. S. J. Cavanagh *et al.*, *Phys. Rev. A* **76**, 052708 (2007).
23. C. Hock, J. B. Kim, M. L. Weichman, T. I. Yacovitch, D. M. Neumark, *J. Chem. Phys.* **137**, 244201 (2012).
24. L. Guo, H. Han, J. Ma, H. Guo, *J. Phys. Chem. A* **119**, 8488–8496 (2015).
25. J. Cooper, R. N. Zare, *J. Chem. Phys.* **48**, 942–943 (1968).
26. S. Boyé-Péronne, D. Gauyacq, J. Liévin, *J. Chem. Phys.* **141**, 174317 (2014).
27. K. M. Ervin, W. C. Lineberger, *J. Phys. Chem.* **95**, 1167–1177 (1991).
28. R. Dressler, M. Allan, *J. Chem. Phys.* **87**, 4510–4518 (1987).
29. D. Hanstorp, C. Bengtsson, D. J. Larson, *Phys. Rev. A* **40**, 670–675 (1989).

ACKNOWLEDGMENTS

The experimental part of this research was funded by the Air Force Office of Scientific Research (FA9550-16-1-0097 to D.M.N.) and the Australian Research Council Discovery Project (DP160102585 to S.T.G.). M.L.W. thanks the National Science Foundation for a graduate research fellowship. Experimental data are available in the supplementary materials. Theoretical work was funded by the National Natural Science Foundation of China (91441107 to J.M.), the Air Force Office of Scientific Research (FA9550-15-1-0305 to H.G.), and the National Science Foundation (CHE-1361121 to D.R.Y.). R.W.F. gratefully acknowledges the Department of Energy, Office of Science, Chemical Sciences Geosciences and Biosciences Division of the Basic Energy Sciences Office (DE-FG0287ER13671). W.C.L. thanks the National Science Foundation JILA Physics Frontier Center (PHY1128544), and G.B. acknowledges the Spanish Ministry of Economy and Competitiveness (EEBB-I-16-11350 and BES-2013-063562).

SUPPLEMENTARY MATERIALS

www.sciencemag.org/content/358/6361/336/suppl/DC1
Materials and Methods
Supplementary Text
Figs. S1 to S12
Tables S1 to S3
Data S1
References (*30*–*62*)

23 June 2017; accepted 29 August 2017
10.1126/science.aao1905

Encoding of vinylidene isomerization in its anion photoelectron spectrum

Jessalyn A. DeVine, Marissa L. Weichman, Benjamin Laws, Jing Chang, Mark C. Babin, Garikoitz Balerdi, Changjian Xie, Christopher L. Malbon, W. Carl Lineberger, David R. Yarkony, Robert W. Field, Stephen T. Gibson, Jianyi Ma, Hua Guo and Daniel M. Neumark

Science **358** (6361), 336-339.
DOI: 10.1126/science.aao1905

The quantum mechanics of a hydrogen hop

Hydrogen migration between adjacent carbons is widespread in the reaction mechanisms of organic chemistry. DeVine *et al.* used photoelectron spectroscopy to discern the quantum mechanical underpinnings of this 1,2 shift in a prototypical case: conversion of vinylidene (H_2CC) to acetylene (HCCH). The technique probed specific states of vinylidene by ejecting electrons with varying energies from a negative ion precursor. Experimental data and accompanying theoretical simulations pinpointed a vibrational rocking mode that facilitated the migration. Replacement of hydrogen with its heavier deuterium isotope disrupted this pathway.

Science, this issue p. 336